

# Here Comes Trebuchet - Optimizing the Counterweight Trebuchet for Maximum Range

Thomas Corie, Jared Park, and David Standring

**Abstract**—We performed an optimization on the design of a counterweight trebuchet with a fixed footprint, or projected area. For this project, we used research performed by others, re-deriving the equations of motion ourselves, to find the best design for throwing a set projectile the greatest distance. Design variables were short arm length, sling length, weight rope length, swing clearance, starting angle and release angle. The constraints were the footprint, the height of the pivot, and the weight position, and we chose the mass of the counterweight and the mass of the projectile. We also included drag on the projectile and built a full-size model of the optimized trebuchet to get real-world data and validate our model. The optimized design launched the projectile 26.8 meters and validated our model to within an error of 6.3%.

**Keywords**—Trebuchet, optimization, projectile.

## I. INTRODUCTION

The trebuchet was a siege weapon used in the Middle Ages to fire projectiles great distances. The counterweight design was a larger, more powerful, and more accurate upgrade to the traction trebuchet, which was powered by a human team pulling on ropes [1]. The counterweight trebuchet came into use in the mid- or late 12th century [1] and was capable of launching 300-pound rocks as far as 300 yards [2]; some sources suggest that medieval trebuchets could launch projectiles as massive as one ton or more [3], [4]. Trebuchets were used until the cannon came into use in the 16th century [3].

The essential components of the trebuchet are the arm, the sling, the pivot, the weight rope, and the counterweight (see Figure 2). Following the approach used in [6], we divided the arm into the long section (Length of Long Arm,  $L_{Al}$ ), nearest the projectile, and short section (Length of Short Arm,  $L_{As}$ ), near the counterweight.

The following abbreviations will be used throughout, and were used in our simulation code (see Figure 3).

### DEFINITIONS

$A_q$	Angle of the arm relative to vertical.
$A_\omega$	Angular velocity of the arm relative to vertical, $\dot{A}_q$ , $A_\omega$ in code and equations.
$D_P$	Diameter of projectile.
$g$	Acceleration due to gravity, $9.81 \text{ m/s}^2$ , $Grav$ in code and equations.
$h$	Height of pivot - considered “zero in $y$ direction”.
$I_{A3}$	Inertia of arm.
$I_{W3}$	Inertia of counterweight.

All three of the authors are graduate students in the Department of Mechanical Engineering at Brigham Young University, Provo UT.

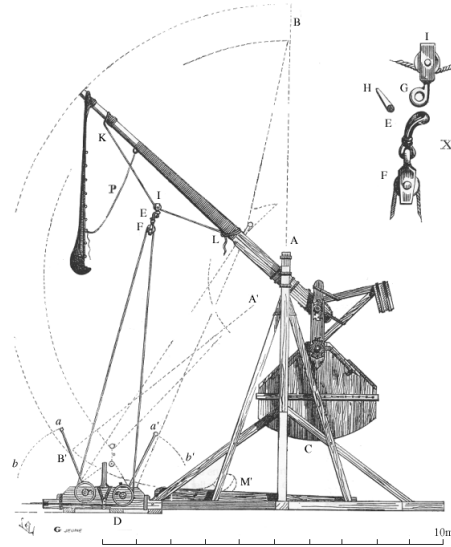


Fig. 1. Diagram of a counterweight trebuchet, from the *Dictionnaire raisonné de l'architecture française du XIe au XVe siècle* (1854-1868) [5].

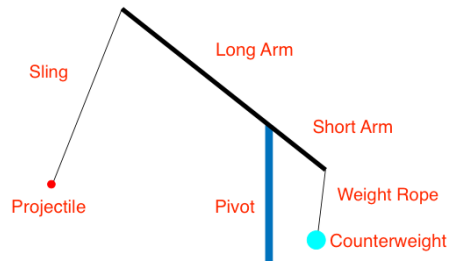


Fig. 2. Parts of the trebuchet.

$L_{A_{cg}}$	Length of arm from pivot to arm COG.
$L_{Al}$	Length of arm from pivot to projectile (“long arm”)
$L_{As}$	Length of arm from pivot to counterweight attachment (“short arm”).
$L_S$	Length of projectile sling.
$L_W$	Length of weight rope.
$m_A$	Mass of arm.
$m_P$	Mass of projectile.
$m_W$	Mass of counterweight.
$S_q$	Angle of the sling relative to arm.
$S_\omega$	Angular velocity of the sling relative to arm, $\dot{S}_q$ , $S_\omega$ in code and equations.

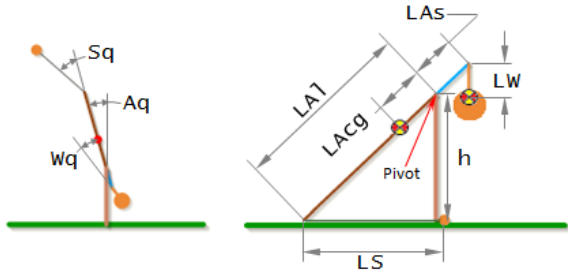


Fig. 3. Parts of trebuchet, using abbreviations, taken from [6].

- $\theta$  Release angle.
- $\theta_0$  Angle of the arm relative to horizontal at  $t = 0$ .
- $Wq$  Angle of the weight relative to arm.
- $W\omega$  Angular velocity of the weight relative to arm,  $\dot{W}q$ ,  $W\omega$  in code and equations.

Despite the trebuchet being a classic engineering problem, our literature review did not find any suggestions for optimizing the dimensions for increased range. There were a number of non-scholarly resources that contained similar information, though they did not provide any derivations or sources for these conclusions. For example, the *Discovery Channel* TV show *MythBusters* constructed a large counterweight trebuchet and stated optimal design parameters that agreed with other sources found on the internet (see Table I) [7], [8], [9].

TABLE I. PURPORTED OPTIMAL DESIGN PARAMETERS

Parameter	Purported Optimal Value
Ratio of $L_{AI} : L_{As}$	3.75:1
Ratio of $L_S : L_{AI}$	1:1
Ratio of $m_W : m_P$	133:1

## II. METHOD

### A. Design Variables and Constraints

Initially the problem had eight design variables that related directly to quantities that had very physical and intuitive meanings. The eight variables, as defined above, were:  $h$ ,  $L_{AI}$ ,  $L_{As}$ ,  $L_S$ ,  $L_W$ ,  $m_A$ ,  $m_W$ , and  $\theta$ . However, after multiple runs of the optimizer, it became clear that  $m_A$  would always go to its lower bound and  $m_W$  would always go to its upper bound. We discovered that it was serving no purpose to include these as design variables, and that they should instead just be set parameters.

We also revised some of the other design variables to be more compatible with the optimizer, though less intuitive in nature. Instead of  $h$ , the design variable was clearance between the weight and ground. The value of  $h$  was then found by adding  $L_{As}$ ,  $L_W$ , and the clearance. This ensured that  $h$  was always taller than the swinging mass, provided that all three design variables were always positive values. We also removed  $L_{AI}$  as a design variable and replaced it with the starting angle of the trebuchet. Early on we had issues with the starting angle

becoming imaginary because  $L_{AI}$  could sometimes be shorter than  $h$ . With the starting angle being the design variable no imaginary angles came up, and  $L_{AI}$  was just calculated from that angle.

Due to the change in design variables, many constraints were automatically resolved, such as the mass not going through the ground. Additionally, we set bounds on all six design variables and set three more inequality constraints. The first constraint limited the footprint to 61 cm (2 ft), and the second limited the overall height to 61 cm. The third constraint ensured that the weight did not rest against the axle before releasing the trebuchet. The bounds are listed below in Table II.

TABLE II. DESIGN VARIABLE BOUNDS

Design Variables	Lower Bound	Upper Bound
$L_{As}$ (cm)	1.0	30.0
$L_W$ (cm)	16.0	45.0
Clearance (cm)	16.0	45.0
$L_S$ (cm)	1.0	61.0
$\theta_0$ (degrees)	10.0	80.0
$\theta$ (degrees)	-80.0	80.0

Following the procedure used in [6], our simulation divides the trebuchet's motion into three stages, each with its own equations of motion (see Figure 4). We used the same nomenclature and variable definitions as [6], but we derived the equations of motion using Lagrange's method, consistent with the method used by [3]. The final equations were consistent.

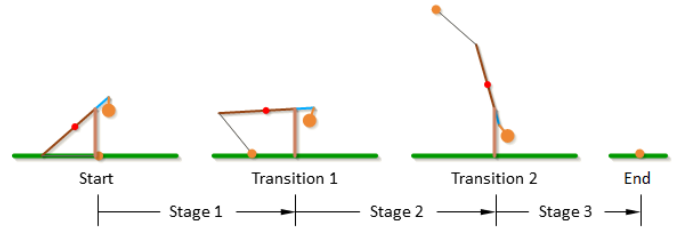


Fig. 4. Stages of trebuchet movement, taken from [6].

### B. Stage 1

In the first section, the trebuchet starts with the sling lying horizontally on the base, with the projectile on the base. We constrained the model to keep the long arm against the base, as this is how we conducted real-world testing.

We used *ode45* in MATLAB with the following state equations:

$$Aq = x_1 \quad (1)$$

$$Wq = x_2 \quad (2)$$

$$Sq = x_3 \quad (3)$$

$$Aw = \dot{A}q = x_4 \quad (4)$$

$$Ww = \dot{W}q = x_5 \quad (5)$$

$$Sw = \dot{S}q = x_6 \quad (6)$$

Using the approach from [6], we arranged the equations of motion into a matrix:

$$\begin{bmatrix} M_{11} & M_{12} \\ M_{21} & M_{22} \end{bmatrix} \begin{bmatrix} \dot{A}w \\ \dot{W}w \end{bmatrix} = \begin{bmatrix} r_1 \\ r_2 \end{bmatrix} \quad (7)$$

where

$$\begin{aligned} M_{11} = & -mP LAI^2 \left(-1 + \frac{2\sin(Aq)\cos(Sq)}{\sin(Aq + Sq)}\right) \\ & + IA3 + IW3 + mA LAcg^2 + \\ & \frac{mP LAI^2 \sin(Aq)^2}{\sin(Aq + Sq)^2} \\ & + mW (LAs^2 + LW^2 + 2 LAs LW \cos(Wq)) \quad (8) \end{aligned}$$

$$M_{12} = IW3 + LW mW (LW + LAs \cos(Wq)) \quad (9)$$

$$M_{21} = IW3 + LW mW (LW + LAs \cos(Wq)) \quad (10)$$

$$M_{22} = IW3 + mW LW^2 \quad (11)$$

$$\begin{aligned} r_1 = & Grav LAcg mA \sin(Aq) + LAI LS mP \\ & (\sin(Sq) (Aw + Sw)^2 + \cos(Sq) (\cos(Aq + Sq) \\ & Sw (Sw + 2 Aw)/\sin(Aq + Sq) + \\ & (\cos(Aq + Sq)/\sin(Aq + Sq) + LAI \cos(Aq) \\ & / (LS \sin(Aq + Sq))) Aw^2)) + \\ & LAI mP \sin(Aq) (LAI \sin(Sq) Aw^2 \\ & - LS (\cos(Aq + Sq) Sw (Sw + 2 Aw)/\sin(Aq + Sq) \\ & + (\cos(Aq + Sq)/\sin(Aq + Sq) + LAI \cos(Aq) \\ & / (LS \sin(Aq + Sq))) Aw^2)) / \sin(Aq + Sq) \\ & - Grav mW (LAs \sin(Aq) + LW \\ & \sin(Aq + Wq)) - LAs LW mW \sin(Wq) \\ & (Aw^2 - (Aw + Ww)^2) \quad (12) \end{aligned}$$

$$\begin{aligned} r_2 = & -LW mW (Grav \sin(Aq + Wq) \\ & + LAs \sin(Wq) Aw^2) \quad (13) \end{aligned}$$

After solving, this produced the following equations for the derivatives of the states:

$$\dot{x}_1 = Aw \quad (14)$$

$$\dot{x}_2 = Ww \quad (15)$$

$$\dot{x}_3 = Sw \quad (16)$$

$$\dot{x}_4 = \dot{A}w = \frac{(r_1 M_{22} - r_2 M_{12})}{(M_{11} M_{22} - M_{12} M_{21})} \quad (17)$$

$$\dot{x}_5 = \dot{W}w = -\frac{(r_1 M_{21} - r_2 M_{11})}{(M_{11} M_{22} - M_{12} M_{21})} \quad (18)$$

$$\begin{aligned} \dot{x}_6 = \dot{S}w = & -\frac{\cos(Aq + Sq) Sw (Sw + 2 Aw)}{\sin(Aq + Sq)} \\ & - \left( \frac{\cos(Aq + Sq)/\sin(Aq + Sq) + LAI \cos(Aq)}{LS \sin(Aq + Sq)} \right) Aw^2 \\ & - \frac{(LAI \sin(Aq) + LS \sin(Aq + Sq)) \dot{x}_4}{LS \sin(Aq + Sq)} \quad (19) \end{aligned}$$

As the stage progresses, the projectile is dragged along the base, and the simulation ends this stage once the projectile leaves the base. This was done by terminating this stage once the condition in Equation 20 was no longer satisfied.

$$F_y < 0 \quad (20)$$

where

$$\begin{aligned} F_y = m_P \left( Grav + \right. \\ \left. \left[ \left( LS \left( \frac{\cos(Aq + Sq) Sw (Sw + 2 Aw)}{\sin(Aq + Sq)} + \right. \right. \right. \right. \\ \left. \left. \left( \frac{\cos(Aq + Sq)}{\sin(Aq + Sq)} + \frac{LAI \cos(Aq)}{(LS * \sin(Aq + Sq))} \right) Aw^2 \right) \right. \right. \\ \left. \left. - LAI \sin(Sq) Aw^2 - LAI (\cos(Sq) - \right. \right. \\ \left. \left. \frac{\sin(Aq)}{\sin(Aq + Sq)} \right) \dot{A}w \right) \right] \sin(Aq + Sq) \left. \right) \quad (21) \end{aligned}$$

### C. Stage 2

The second stage of the simulation tracks the progress of the projectile from the point where it leaves the ground, to where it is released from the trebuchet. The initial values of Stage 2 are the final values calculated in Stage 1, with the state equations passed to *ode45* following the same order as Stage 1 (Equations 1 - 6). Note that Stage 2 has three degrees of freedom, since *Sw* is allowed to change independent of other variables.

The equations of motion were arranged into a matrix:

$$\begin{bmatrix} M_{11} & M_{12} & M_{13} \\ M_{21} & M_{22} & 0 \\ M_{31} & 0 & M_{33} \end{bmatrix} \begin{bmatrix} \dot{A}w \\ \dot{W}w \\ \dot{S}w \end{bmatrix} = \begin{bmatrix} r_1 \\ r_2 \\ r_3 \end{bmatrix} \quad (22)$$

where

$$\begin{aligned} M_{11} = & IA3 + IW3 + mA LAcg^2 + \\ & mP (LAI^2 + LS^2 + 2 LAI LS \cos(Sq)) + \\ & mW (LAs^2 + LW^2 + 2 LAs LW \cos(Wq)) \quad (23) \end{aligned}$$

$$M_{12} = IW3 + LW mW (LW + LAs \cos(Wq)) \quad (24)$$

$$M_{13} = LS mP (LS + LAI \cos(Sq)) \quad (25)$$

$$M_{21} = IW3 + LW mW (LW + LAs \cos(Wq)) \quad (26)$$

$$M_{22} = IW3 + mW LW^2 \quad (27)$$

$$M_{31} = Ls mP (LS + LA1 \cos(Sq)) \quad (28)$$

$$M_{33} = mP LS^2 \quad (29)$$

$$\begin{aligned} r_1 = & Grav LAcg mA \sin(Aq) + \\ & Grav mP (LAl SIN(Aq) + LS \sin(Aq + Sq)) - \\ & Grav mW (LAs \sin(Aq) + LW \sin(Aq + Wq)) - \\ & LAl LS mP \sin(Sq) (Aw^2 - (Aw + Sw)^2) - \\ & LAs LW mW \sin(Wq) (Aw^2 - (Aw + Ww)^2) \quad (30) \end{aligned}$$

$$r_2 = -L mW (Grav \sin(Aq) + Wq) + LAs SIN(Wq) Aw^2 \quad (31)$$

$$r_3 = LS mP (Grav \sin(Aq + Sq) - LAl \sin(Sq) Aw^2) \quad (32)$$

Returning to Equation 22, performing matrix division to both sides of the equation allows for  $\dot{A}_w, \dot{W}_w,$  and  $\dot{S}_w$  to be found. In the equation below,  $[dots]$  refers to the vertical matrix of the derivatives ( $\dot{A}_w, \dot{W}_w,$  and  $\dot{S}_w$ ),  $[M]$  refers to the 3x3 matrix, and  $[r]$  refers to the column vector of  $r_1, r_2$  and  $r_3$ .

$$[dots] = [M] \setminus [r] \quad (33)$$

Stage 2 continues in the *ode45* function until the projectile is traveling along the release angle. This is done using an stop event in the *ode45* options.

#### D. Stage 3

Stage 3 is projectile motion. The initial velocity vector is calculated from the final angular velocities at the end of Stage 2 with the following two equations:

$$v_x = -L_{Al} A_w \cos(A_q) - L_S (A_w + S_w) \cos(A_q + S_q) \quad (34)$$

$$v_y = -L_{Al} A_w \sin(A_q) - L_S (A_w + S_w) \sin(A_q + S_q) \quad (35)$$

The trajectory is then calculated using *ode45* until the projectile hits the ground. Using *ode45* was necessary because we included drag on the projectile, otherwise simple algebra could be used to calculate the throw distance. This stage has a new set of state variables:

$$d_x = x_1 \quad (36)$$

$$d_y = x_2 \quad (37)$$

$$v_x = x_3 \quad (38)$$

$$v_y = x_4 \quad (39)$$

where  $d_x$  and  $d_y$  are positions, and  $v_x$  and  $v_y$  are velocities. The corresponding ODEs are:

$$\dot{x}_1 = x_3 \quad (40)$$

$$\dot{x}_2 = x_4 \quad (41)$$

$$\dot{x}_3 = -\frac{\rho C_d A_{eff} (x_3 - WS)}{(2 mP)} \sqrt{x_4^2 + (WS - x_3)^2} \quad (42)$$

$$\dot{x}_4 = -Grav - \frac{\rho C_d A_{eff} x_4}{(2 mP)} \sqrt{x_4^2 + (WS - x_3)^2} \quad (43)$$

where  $\rho$  is the density of air,  $C_d$  is the coefficient of drag on the projectile,  $A_{eff}$  is the effective area of the projectile, and  $WS$  is the wind speed. We used experimental data taken from [10] to calculate the coefficient of drag. The coefficient of drag varies with the Reynolds number and had to be calculated at each time step in each iteration.

### III. RESULTS

The objective function, which calculated the range, or final distance in the  $x$  direction reached by the projectile, was optimized using MATLAB's built-in optimizer *fmincon* with its *active-set* algorithm. The best results were achieved by first running a particle swarm algorithm to warm start the *fmincon* optimizer. The solution resulted in a throw distance of 35.9 meters. The optimal values for the design variables had to be translated into the actual design parameters. This optimal distance is achieved when the long arm is 70.06 cm, the short arm is 24.05 cm, the sling is 61.00 cm, the weight rope is 19.37 cm, the pivot point is 59.42 cm tall, and the release angle is 43.4 degrees (see Table III).

TABLE III. OPTIMIZATION RESULTS

Design Parameters	Optimal Value
$L_{Al}$ (cm)	70.06
$L_{As}$ (cm)	24.05
$L_S$ (cm)	61.00
$L_W$ (cm)	19.37
$h$ (cm)	59.42
$\theta$ (degrees)	43.4

As the constraints have evolved, it was interesting to see that the release angle did not always result in 45 degrees as defined, which is relative to the arm. However, the release angle was generally very close to 45 degrees from the vertical. This is logical, because with simple projectile motion the maximum distance is achieved with an initial trajectory at 45 degrees. Therefore, the optimal trebuchet throw would be achieved when the velocity of the projectile is at 45 degrees to the vertical. Depending on the design of the trebuchet, the projectile is released with the arm at various angles. The release angle then needs to compliment the final arm angle so the combined angle is 45 degrees to the vertical. This is what was seen in the optimal solution.

Table IV shows how closely our design agreed with the suggestions found through various sources in our initial research. The ratio of the long and short arms was close to that given as optimal. The sling length to long arm length ratio was limited due to our footprint constraint, and would always result in a design at the constraint.

TABLE IV. RESULTS COMPARED TO PURPORTED OPTIMAL PARAMETERS

Parameter	Purported Optimal Value	Optimization Result
Ratio of $L_{AI} : L_{As}$	3.75:1	2.91:1
Ratio of $L_S : L_{AI}$	1:1	0.87:1*
Ratio of $m_W : m_P$	133:1	143:1†

\*at constraint limit  
 † chosen for design

The counterweight we chose to use, a 6.5 kg exercise weight, and the 45.6 g golf ball projectile resulted in a ratio close to that suggested as optimal. Initial optimizations using the ratio of the counterweight mass to projectile mass agreed with our intuition, i.e. a greater counterweight mass results in a greater range. This suggests that a given design should use the largest counterweight possible without risking mechanical failure.

#### IV. MODEL VERIFICATION

Verification of the model was performed by constructing a prototype trebuchet based on dimensions produced by the optimization program. The cross sectional area of the swing arm was chosen due to material constraints and loaded into the program, causing the rotational inertia and mass to be functions of the length of the arm. The footprint of the trebuchet was added as a constraint to the optimization program, which was then run to find an optimal design.

A simple trebuchet was built as shown in Figure 5. The axle was constructed with a wooden dowel, with PVC piping used as a bushing. A 3D printed “sled” (Figure 6) was designed to hold the projectile, with parachute chord used as a sling.



Fig. 5. Prototype constructed for verification of the model.



Fig. 6. 3D printed “sled” to hold the projectile.

The trebuchet was fired multiple times and its release pin was modified by hand until its range appeared to be at a maximum. A high speed camera (240 fps) was then used to record the trebuchet during launch. The achieved range was then recorded and it was compared to the model’s results. The model predicted that the trebuchet would fire the projectile 35.9m, while the prototype fired a maximum 26.8m. This gives an error of 25%. Upon review of the video, we noticed that the trebuchet prototype was actually releasing at 61 degrees. This release angle was fed back into the simulator and the predicted throw distance was 28.6m, resulting in 6.3% error. The predicted release position was also very comparable to that of the prototype (see Figure 7). If more precise tuning methods were known the release angle could have better matched the model and most likely caused an increase in range. Further deviation from the model can be attributed to energy losses in the simple design. Friction of the axle, interference between the weight and the arm when shooting, and the tendency of the trebuchet to jump forward; all caused energy losses in the system. During testing, it was also observed that the test trajectory was facing a slight uphill grade, and there was a noticeable headwind.

The error is relatively low, and does lend credence to the model, but a more accurate model can be constructed to include those losses. A more robust prototype could be constructed to avoid inefficiencies in the design, and better match the mathematical model. An optimizer that takes into account the uncertainty in a real trebuchet, especially in the release angle, would also more closely model the real behavior.

#### V. CONCLUSION

We optimized the design of a counterweight trebuchet with a fixed footprint, or projected area, with range as the objective. We built off of work performed by others (re-deriving the equations for verification) and showed that the best design for throwing a set projectile the greatest distance did follow the guidelines produced by non-academics fairly closely. Our design variables were swing arm length, sling length, weight rope length, pivot height, and release angle. The constraints

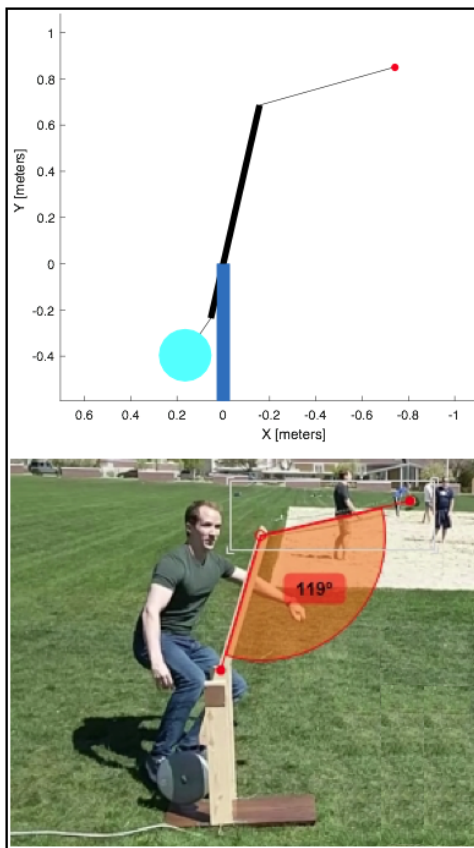


Fig. 7. Release position of the simulation compared to the prototype. The measured angle on the prototype is the supplementary angle of the release angle.

were the footprint, and the height of the pivot, with a set counterweight mass and projectile mass. We included drag on the projectile and built a full-size model of the optimized trebuchet to validate our model. The optimized design had a range of 26.8 meters.

## REFERENCES

- [1] W. T. S. Tarver, "The Traction Trebuchet - A Reconstruction of An Early-Medieval Siege Engine," *Technology and Culture*, vol. 36, no. 1, pp. 136–167, jan 1995.
- [2] L. O'Connor, "Building a better trebuchet." *Mechanical Engineering*, vol. 116, no. 1, p. 66, jan 1994.
- [3] M. Denny, "Siege engine dynamics," *European Journal of Physics*, vol. 26, no. 4, p. 561, 2005. [Online]. Available: <http://stacks.iop.org/0143-0807/26/i=4/a=002>
- [4] P. E. Chevedden and L. Eigenbrod, "The Trebuchet," *Scientific American*, vol. 273, no. 1, pp. 66–71, 1995.
- [5] E. Viollet-le Duc, "Fonctionnement d'un trébuchet, engin militaire du Moyen-Âge." [Online]. Available: <https://commons.wikimedia.org/wiki/File:Trebuchet2.png>
- [6] E. Olson and P. Olson, "VirtualTrebuchet," 2013. [Online]. Available: <http://www.virtualtrebuchet.com/>
- [7] S. Christiansen, "Episode 248 - Duct Tape Trebuchet," 2016. [Online]. Available: <http://www.sciencechannel.com/tv-shows/mythbusters/videos/how-to-build-a-trebuchet/>

- [8] J. Hall, "Trebuchet Physics," 2008. [Online]. Available: <http://www.stormthecastle.com/trebuchet/trebuchet-physics.htm>
- [9] M. Senese, "Tuning A Trebuchet For Maximum Distance - A Look at the Components and Variables," 2010. [Online]. Available: <http://www.mikesenese.com/DOIT/2010/12/tuning-a-trebuchet/>
- [10] R. Mehta and J. Pallis, "Sports Ball Aerodynamics: Effects of Velocity, Spin and Surface Roughness," 2001. [Online]. Available: <http://iweb.tms.org/ED/01-5085-185.pdf>